Electronic Supplementary Information for

SO_2 Capture Enhancement in NU-1000 by the Incorporation of a Ruthenium Gallate Organometallic Complex

Jorge García Ponce,[a,†] Mariana L. Díaz-Ramírez,[b,†] Saidulu Gorla,[c] Chanaka Navarathna,[c,†] Gabriela Sanchez-Lecuona,[c,†] Bruno Donnadieu,[c] Ilich A. Ibarra*,[b] and Virginia Montiel-Palma*,[c]

[a] Escuela Moderna Americana, Cerro del Hombre 18, Romero de Terreros, Coyoacan 04310, Ciudad de México, Mexico.

[b] Laboratorio de Fisicoquímica y Reactividad de Superficies (LaFReS), Instituto de Investigaciones en Materiales, Universidad Nacional Autónoma de México, Circuito Exterior s/n, CU, Coyoacán, 04510, Ciudad de México, Mexico. E-mail: argel@unam.mx

[c] Department of Chemistry, Mississippi State University, Box 9573, Mississippi, 39762, United States. E-mail: vmontiel@chemistry.msstate.edu

Contents

1. General Experimental procedures 3
1.1 Synthesis of $[MeRu(h^6\text{-}C_6H_6)(PPh_3)_2][GaMe_2Cl_2]$ 3
1.2 Synthesis of [RuGa]@NU-1000 4
1.2.1 Ru and Ga determination by ICP-MS 4
1.2.2 XPS analysis 5
2. NMR spectra 11
3. Single crystal X-ray diffraction 14
3.1 Crystal Structure Report for complex **1** 14
4. Powder X-ray Diffraction 24
5. N_2 and SO_2 isotherms 25
6. Heat of adsorption of SO_2 26

1. General Experimental procedures

All experiments were performed either under an argon atmosphere in vacuum atmosphere using standard Schlenk methods or in MBraun glove boxes. Benzene was dried and distilled from sodium using benzophenone ketyl as an indicator. Hexane was and dried by passing through MBraun-SPS column systems. In either case, solvents were degassed prior to use. CD_2Cl_2 was dried by passing through a small column of molecular sieves and alumina and stored over 4 Å molecular sieves in the glovebox. Compound $[Ru(PPh_3)_3Cl_2]$ was prepared according to literature methods.[1] $GaMe_3$ was purchased from Strem Chemicals Inc. and used as received. Nuclear magnetic resonance (NMR) experiments were performed on Bruker Avance 300MHz, and Bruker Avance 500MHz spectrometers operating with frequency, deuterated solvent and temperature indicated in parentheses. Chemical shifts (δ) are reported in parts per million (ppm).

1.1 Synthesis of $[MeRu(\eta^6\text{-}C_6H_6)(PPh_3)_2][GaMe_2Cl_2]$

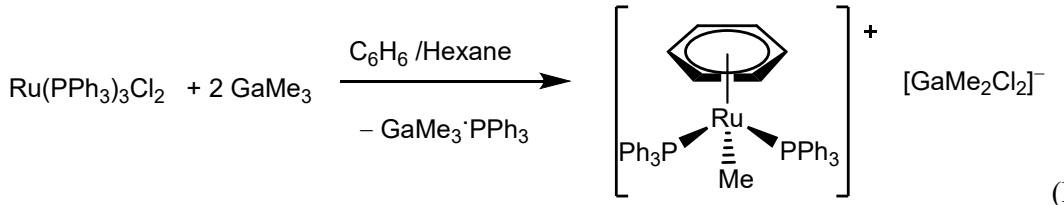

(Eq. S1)

A solution of 2 mL of hexane and $GaMe_3$ (104 µL, 1.025 mmol) was added to a suspension of $[Ru(PPh_3)_3Cl_2]$(500 mg, 0.52 mmol) in 5mL of benzene. This mixture was stirred for 12 h, rendering a yellow suspension which was subsequently filtrated. The yellow solid was washed with hexane (2 × 1 mL), benzene: hexane (1:1) (3 × 1mL), hexane (1 × 1 mL), and dried under vacuum. Isolated yield 320 mg (69 %). ^{1}H NMR (600 MHz, Methylene Chloride-d_2) δ 7.46 – 7.39 (m, 5H, C_{arom}), 7.36 (s, 3H, C_{arom}), 7.33 – 7.27 (m, 11H, C_{arom}), 7.12 (ddt, J = 8.5, 5.3, 3.0 Hz, 11H, C_{arom}), 5.47 (s, 6H, C_{arene}), 1.26 (t, J_{PH} = 6.2 Hz, 3H, CH_3-Ru), -0.20 (s, 6H, CH_3-Ga). $^{13}C^2$ NMR (151 MHz, Methylene Chloride-d_2) δ 135.4 – 134.6 (m, C_{arom}), 134.2 (t, J_{CP} = 4.6 Hz, C_{arom}), 131.2, 129.0 (t, J_{CP}= 4.9 Hz, C_{arom}), 128.8, 97.6 (t, J_{CP} = 2.7 Hz, C_{arene}), 0.34 (s, CH_3-Ga) -17.0 (t, J_{CP} = 14.9 Hz, CH_3-Ru). ^{31}P NMR (202 MHz, Chloroform-d) δ 35.0 (s). Anal. Calcd. for $C_{45}H_{45}Cl_2GaP_2Ru\cdot1.7C_6H_6$: C: 64.86%, H: 5.44%; Found: C: 64.86, H: 5.52.

1.2 Synthesis of [RuGa]@NU-1000

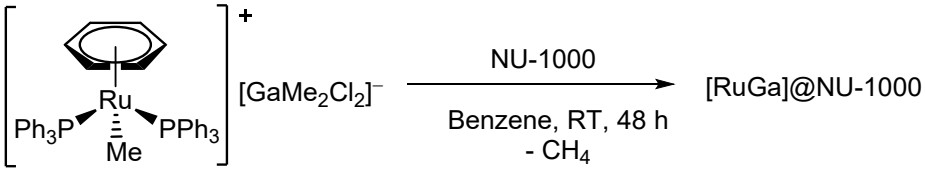

(Eq. S2)

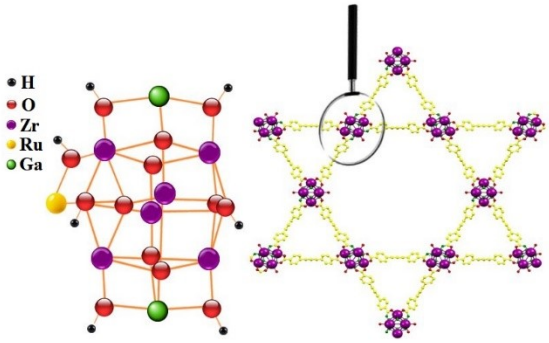

Scheme S1. Material [RuGa]@NU-1000: (Left) A representation of the Zr_6 node of NU-1000 material (right) grafted with complex **1**.

Microcrystalline NU-1000 (146 mg, 0.07 mmol) was added to a 50 mL benzene solution of $[MeRu(h^6\text{-}C_6H_6)(PPh_3)_2][GaMe_2Cl_2]$ (155 mg, 0.175 mmol) at room temperature. After stirring for 48 h, the heterogeneous mixture was filtered using a fine porosity glass frit. The resulting solids were washed with small amounts of benzene (~ 10 mL). The solids were soaked overnight in 10 mL benzene and washed with fresh benzene (4 × 1 mL) and pentane (5 × 1 mL). The overnight soaking and rinsing procedure was repeated once more. Finally, the solids were dried under dynamic vacuum for 12 h. Yield: quantitative. ICP-MS: Ru 1.21%, Ga 1.79 wt. %. Consistent with a Ru : Ga molar ratio of 1 : 2.1.

1.2.1 Ru and Ga determination by ICP-MS

The metal content in [RuGa]@NU-1000 solutions was measured by inductively coupled plasma-mass spectrometer (ICP-MS). The ICP-MS calibration curves were obtained with a series of standardized ruthenium, gallium and zirconium solutions, where ruthenium (III) chloride hydrate (Certipur ICP standard from Sigma Aldrich); and gallium trichloride and zirconium tetrachloride (CRM standards from Sigma Aldrich) were treated with mixture of conc. H_2SO_4 (40µL), DMSO (3 mL) and 18 MΩ.cm Nanopure water (0.96 mL). The desired standardized solutions were prepared by diluting aliquot of stock solution to a final volume of 10 mL of the same matrix. To perform ICP-MS for [RuGa]@NU-1000, samples were dissolved in conc. H_2SO_4 until full dissolution, DMSO and 18 MΩ.cm Nanopure water.

The technique gave the values of weight percent content of each of the metals given below. Conversion to mol gave an approximate molar ratio of one Ru atom and 2 Ga atoms per Zr_6 unit.

	Ru	Ga	Zr
Found w%	1.78	2.95	11. 8
n/100g sample:	0.0176 mol	0.0423 mol	0.129 mol
Molar ratio	0.816	1.96	6.00
Approximate molar ratio	1	2	6

1.2.2 XPS analysis

Low resolution (LR)-XPS scan spectra of NU-1000, $[MeRu(h^6\text{-}C_6H_6)(PPh_3)_2][GaMe_2Cl_2]$ and [RuGa]@NU-1000 are shown in Figure 1 and Table 1. NU-1000 has its characteristic elements C (74.1 %), O (21.27 %) and Zr (3.3 %). Ga, Ru, C, O, Cl and P were present in $[MeRu(\eta^6\text{-}C_6H_6)(PPh_3)_2][GaMe_2Cl_2]$ confirming the successive formation of the precursor. [RuGa]@NU-1000 had Ga, C, O and Zr. However, the signal intensity was too accurately detect Ru, Cl and P in LR-XPS. It should be noted that XPS is a very surface sensitive method with the predominant contribution of the signals arising from the outer 10 Å region of the surface and may not represent the bulk composition.

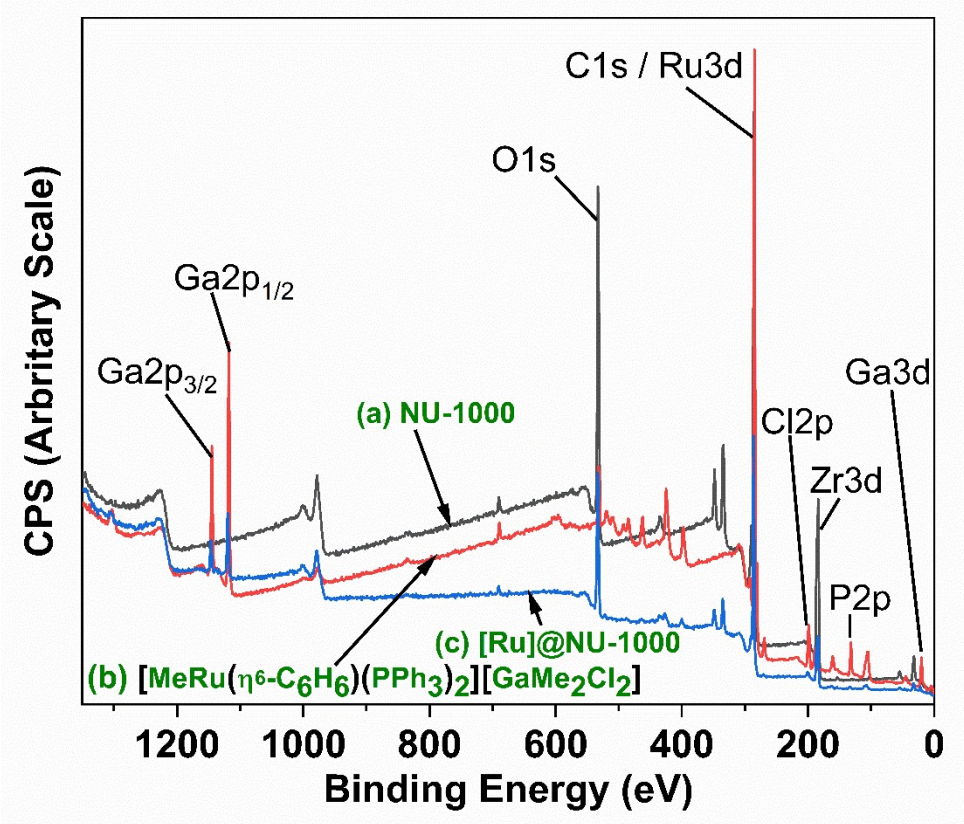

Figure S1. Low resolution (LR) wide scan survey spectra for a)NU-1000, b) [MeRu(h^6-C_6H_6)(PPh_3)$_2$][$GaMe_2Cl_2$] and [RuGa]@NU-1000

Table S1. Low resolution (LR) wide scan survey spectra data for a) NU-1000, b) [MeRu(h^6-C_6H_6)(PPh_3)$_2$][$GaMe_2Cl_2$] and [RuGa]@NU-1000

	(a)		(b)		(c)	
	Peak BE (eV)	Atomic %	Peak BE (eV)	Atomic %	Peak BE (eV)	Atomic %
C1s	285.82	74.1	285.04	79.3	286.18	73.19
O1s	532.78	21.27	531.96	4.82	533.21	21.85
Zr3d	184.5	3.3	-	-	185.05	2.34
Ga3d	-	-	20.09	3.42	21.91	0.92
Ru3d	-	-	285.03	5.43	-	-
Cl2p	-	-	199.04	2.44	-	
P2p	-	-	132.05	3.25	-	-

The Ga2p, Ru3d, Zr3d, C1s, O1s, P2p and Cl2p HR-XPS spectra of NU-1000, [MeRu(h^6-C_6H_6)(PPh_3)$_2$][$GaMe_2Cl_2$] and [RuGa]@NU-1000 each resolved and displayed in Figure 2 and Table 2.

The NU-1000 MOF shows its characteristic Zr3d, C1s and O1s HR-XPS spectra patterns, as previously reported.[3 4]

The Ga2p HR-XPS for the [RuGa]@NU-1000 exhibits a binding energy shift to 1118.82 eV from 1117.91 eV. Also, the atomic % M-O or M-O-M has increased to 6.96 % versus the precursors [(a) 2.73 % and (b) 1.63 %]. This is evident for the formation of Ga-O-Zr or Ru-O-Zr bonds.[5, 6] Further, Zr-O atomic percentage of Zr3d HR-XPS has decreased to 2.8 % from 3.7 % which may also can be attributed decrease in Zr-O or Zr-O-Zr functionality. However, their relative composition in the final material may need to be considered for a better comparison.

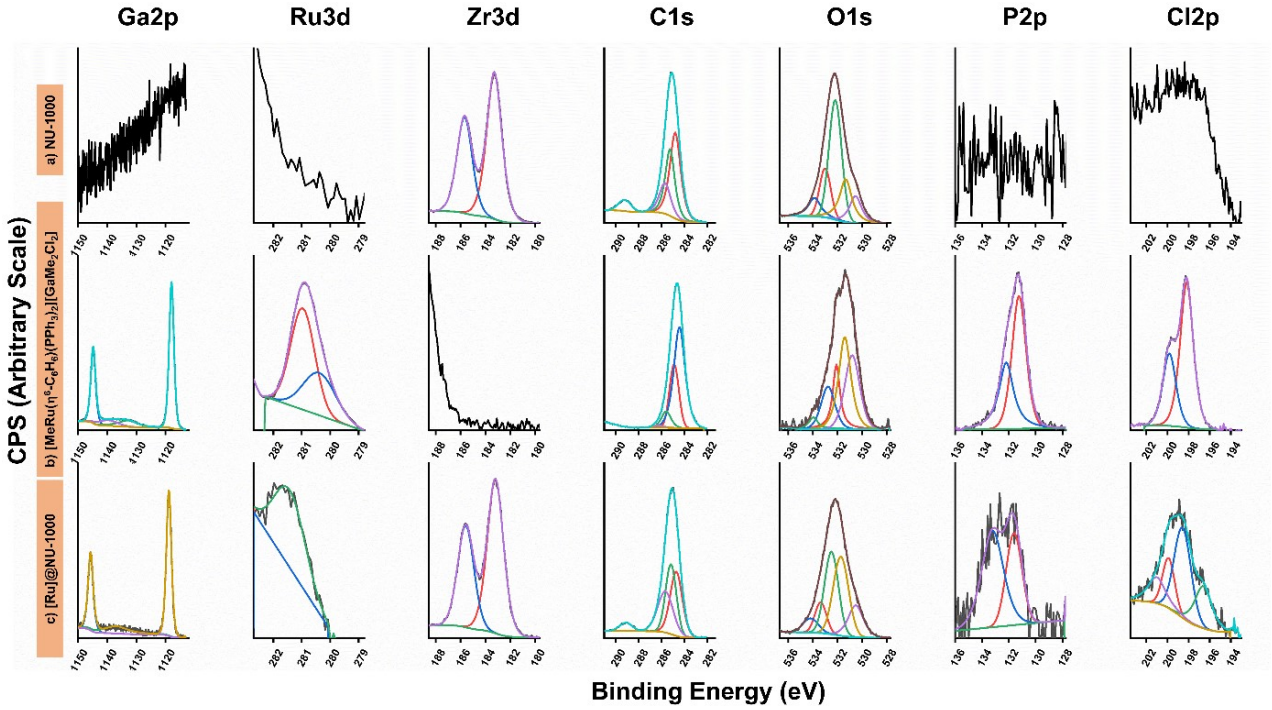

Figure S2. High resolution (HR XPS) spectra Ga2p, Ru3d, Zr3d, C1s, O1s, P2p and Cl2p spectra for NU-1000, $[MeRu(h^6\text{-}C_6H_6)(PPh_3)_2][GaMe_2Cl_2]$ and [RuGa]@NU-1000

Table S2: High resolution (HR XPS) data Ga2p, Ru3d, Zr3d, C1s, O1s, P2p and Cl2p spectra for NU-1000, $[MeRu(h^6\text{-}C_6H_6)(PPh_3)_2][GaMe_2Cl_2]$ and [RuGa]@NU-1000. **Note that certain binding energy assignments are based on electronegativity differences due to the unavailability of Ru/Ga reference compound data. The BE values were estimated with a maximum error of ±0.05 eV in curve fitting.*

	Peak		(a)	(b)	(c)
$Ga2p_{1/2}$	-Ga-R/-Ga-O	BE (eV)	-	1139.69	-
		Atomic %	-	0.78	-
		FWHM (eV)	-	8	-
$Ga2p_{3/2}$	-Ga-R/-Ga-O	BE (eV)	-	1117.91	1118.82
		Atomic %	-	5.08	1.55
		FWHM (eV)	-	1.91	2.02
Ru3d	-Ru-O/-Ru-P	BE (eV)	-	280.97	-
		Atomic %	-	0.98	-
		FWHM (eV)	-	0.99	-
	Ru (metallic)/RuO_x	BE (eV)	-	280.33	-
		Atomic %	-	0.55	-
		FWHM (eV)	-	1.34	-
Zr3d	Zr-O/O-Zr-O	BE (eV)	183.29	-	183.2
		Atomic %	3.7	-	2.8
		FWHM (eV)	1.43	-	1.53
C1s	-COOH(R)	BE (eV)	289.21	-	289.11
		Atomic %	4.64	-	3.28
		FWHM (eV)	1.31	-	1.31
	>C=O	BE (eV)	285.68	286.26	285.65
		Atomic %	12.03	0.99	20.05
		FWHM (eV)	1.15	1.06	1.58
	C-O	BE (eV)	285.24	285.58	285.16
		Atomic %	22.64	6.68	23.54
		FWHM (eV)	0.97	0.99	1.12
	C-C C=C, C-H	BE (eV)	284.78	284.88	284.7
		Atomic %	32.97	23.95	24.82
		FWHM (eV)	1.12	0.96	1.25

		BE (eV)	-	284.42	-
		Atomic %	-	50.01	-
		FWHM (eV)	-	1.16	-
O1s	-COOH(R)	BE (eV)	533.87	533.96	534.19
		Atomic %	1.97	0.19	1.25
		FWHM (eV)	1.18	0.87	1.46
	>C=O	BE (eV)	533	532.77	533.36
		Atomic %	3.93	0.78	2.03
		FWHM (eV)	1.07	1.32	1.1
	C-O	BE (eV)	532.18	532.09	532.49
		Atomic %	10.74	0.83	6.57
		FWHM (eV)	1.2	1.5	1.33
	M-O, M-O-M, M-O-M' (M/M'=Zr, Ga or Ru)	BE (eV)	530.53	531.41	531.73
		Atomic %	2.73	1.63	6.96
		FWHM (eV)	1.18	1.17	1.47
		BE (eV)	-	530.8	530.51
		Atomic %	-	1.47	2.94
		FWHM (eV)	-	1.43	1.44
P2p	-P=O	BE (eV)	-	-	133.21
		Atomic %	-	-	0.34
		FWHM (eV)	-	-	1.91
	-Ru-P	BE (eV)	-	131.24	131.62
		Atomic %	-	3.08	0.65
		FWHM (eV)	-	1.23	1.39
Cl2p	Ga-Cl-Ga	BE (eV)	-	-	201.02
		Atomic %	-	-	0.51
		FWHM (eV)	-	-	1.97

	Ru-Cl-Ga	BE (eV)	-	-	199.89
		Atomic %	-	-	0.57
		FWHM (eV)	-	-	1.35
	Ga-Cl	BE (eV)	-	198.18	198.58
		Atomic %	-	2.98	1.43
		FWHM (eV)	-	1.47	1.88
	Ru-Cl-Ru	BE (eV)	-	-	196.6
		Atomic %	-	-	0.72
		FWHM (eV)	-	-	1.9

1.2.3 SEM-EDX analysis

The new material was subjected to analysis by SEM-EDX (electron images and spectral processing shown below).

It should be remembered that SEM-EDX is a semiquantitative technique for the chemical composition of samples giving information on the elemental composition as well as their distribution and concentration. However, it is mostly focused on the surface layer and therefore the results must be taken with caution.

The values below come from the spectral analysis, where the weight percentage and the atomic percentages are given. The molar ratios between Zr: Ga: Ru are respectively 6 : 1.2: 0.7. These values are lower than those determined by ICP-MS but the discrepancy can be explained due to the SEM-EDX technique focusing on the elements present in the most external layers of the material in contrast to ICP-MS where samples where fully digested. Yet, the ratio between Ga: Ru is approximately 1.7 : 1 (by ICP-MS 2.4 :1) and is consistent.

	w%	Atomic%	atomic ratio (arbitrary)
Ga	11.75	14.98	1.2
Zr	78.08	76.08	6
Ru	10.16	8.94	0.7

Electron images of material RuGa@NU-1000

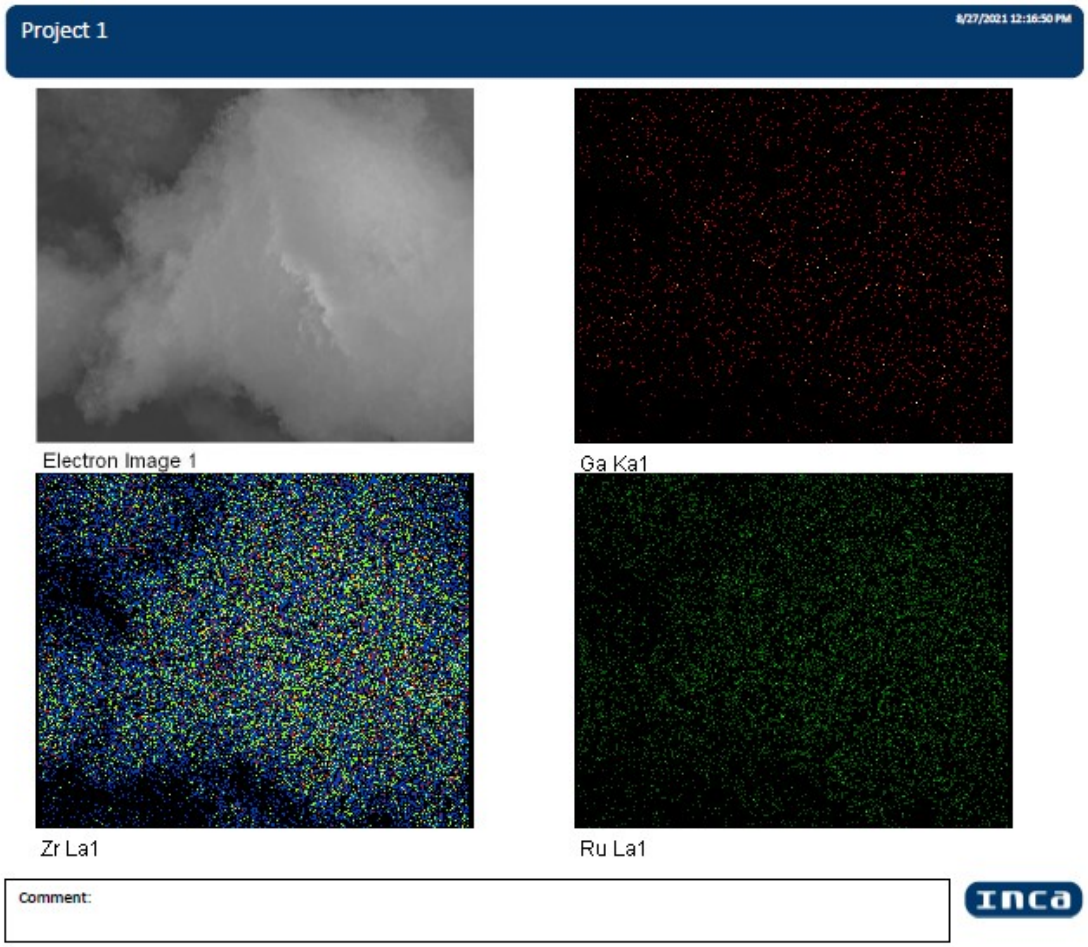

Spectral analysis of material RuGa@NU-1000

Project 1

8/27/2021 12:17:39 PM

Spectrum processing :

Peaks possibly omitted : 0.682, 8.012 keV

Processing option : All elements analyzed (Normalised)

Number of iterations = 3

Standard :

Ga GaP 1-Jun-1999 12:00 AM

Zr Zr 1-Jun-1999 12:00 AM

Ru Ru 1-Jun-1999 12:00 AM

Element	Weight%	Atomic%
Ga K	11.75	14.98
Zr L	78.08	76.08
Ru L	10.16	8.94
Totals	100.00	

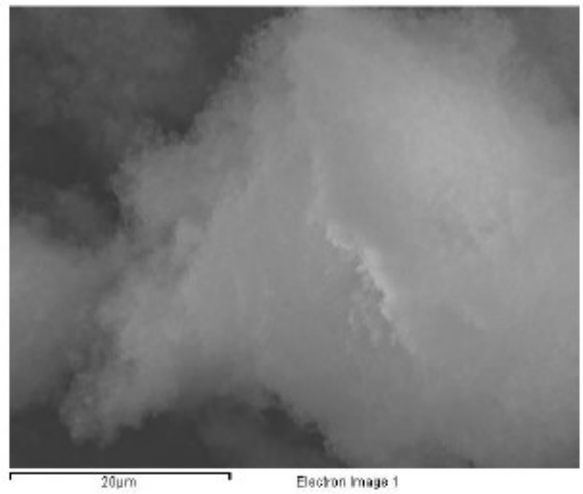

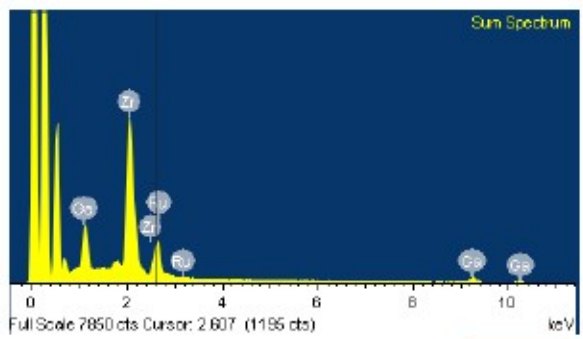

Comment:

1.2.4 TGA analysis

The plot below shows the plots of the thermal gravimetric analysis of the unmodified MOF material NU-1000 and the comparisons with the organometallic precursor non grafted to the MOF and the RuGa@NU-1000 material. It should be noticed that there are no reported TGA plots of the organometallic complex or similar species, however, it can be noticed that the grafted material RuGa@NU-1000 is modified from its parent NU-1000.

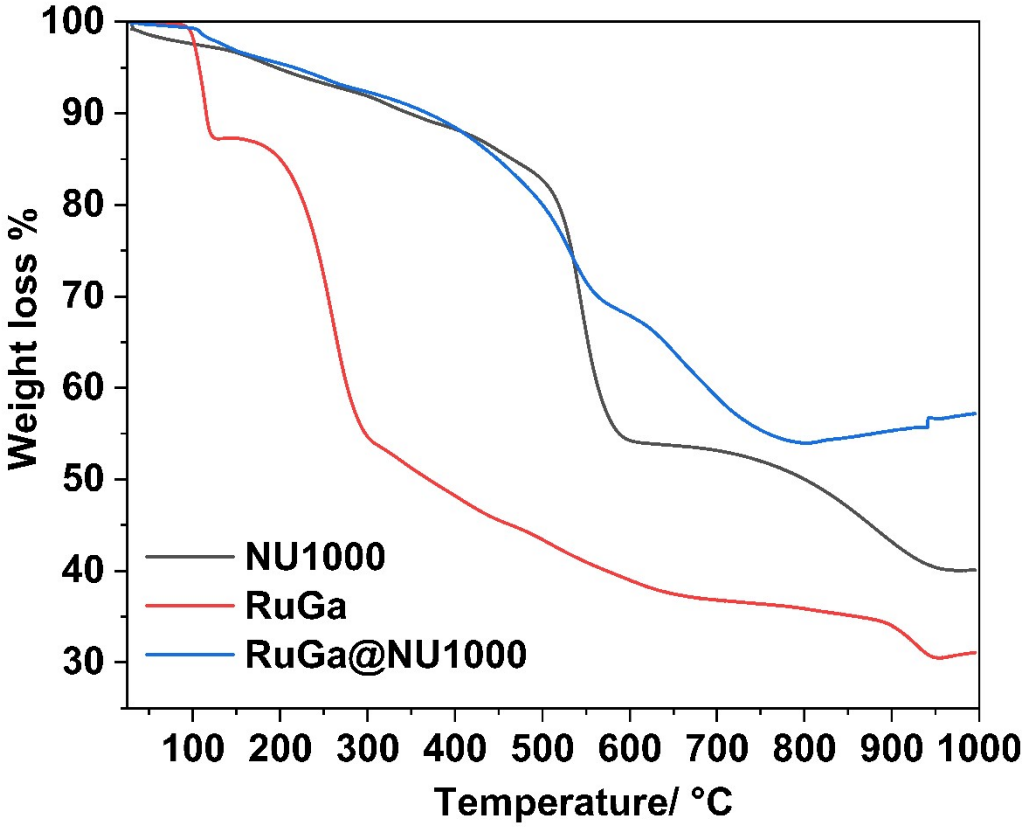

2. NMR spectra

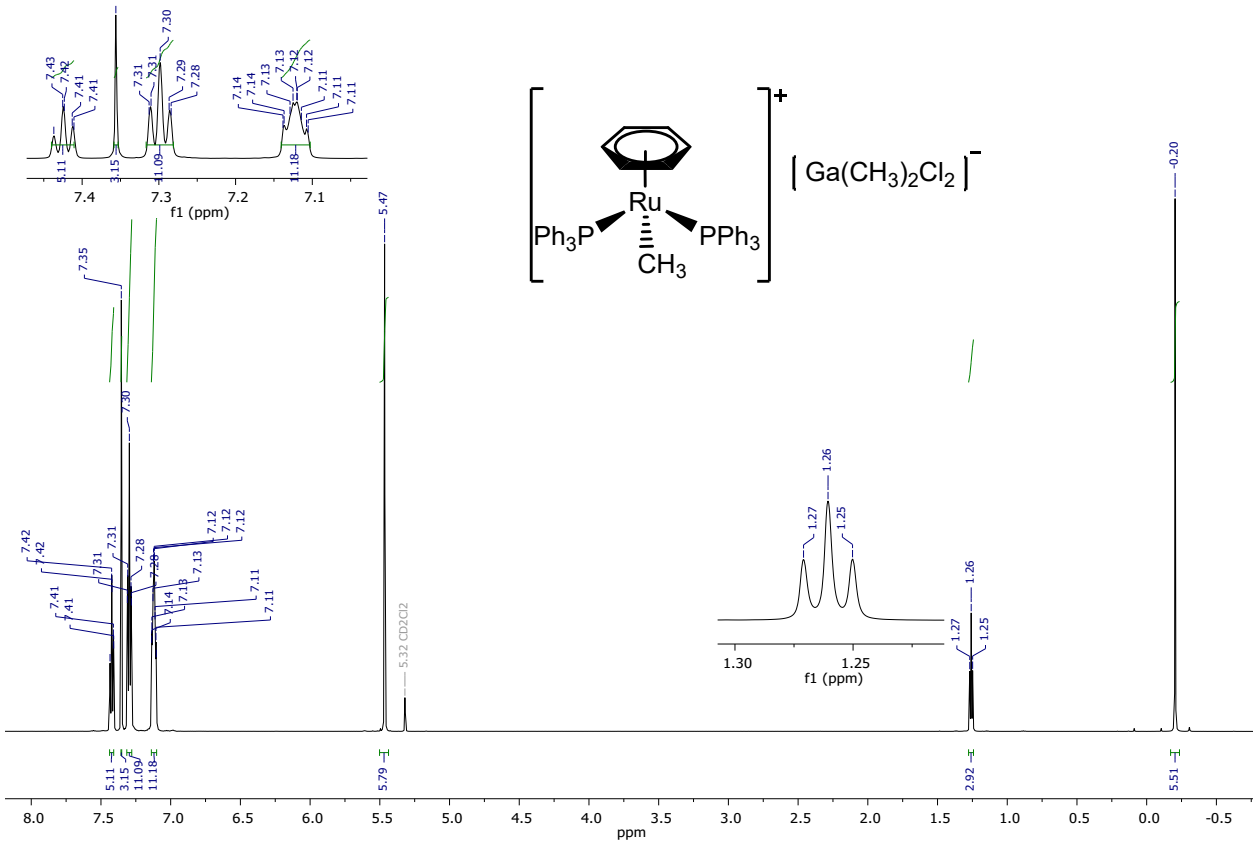

Figure S3. ^{1}H NMR spectrum (600 MHz, CD_2Cl_2, 298 K) of [MeRu(h^6-C_6H_6)(PPh_3)$_2$][$GaMe_2Cl_2$].

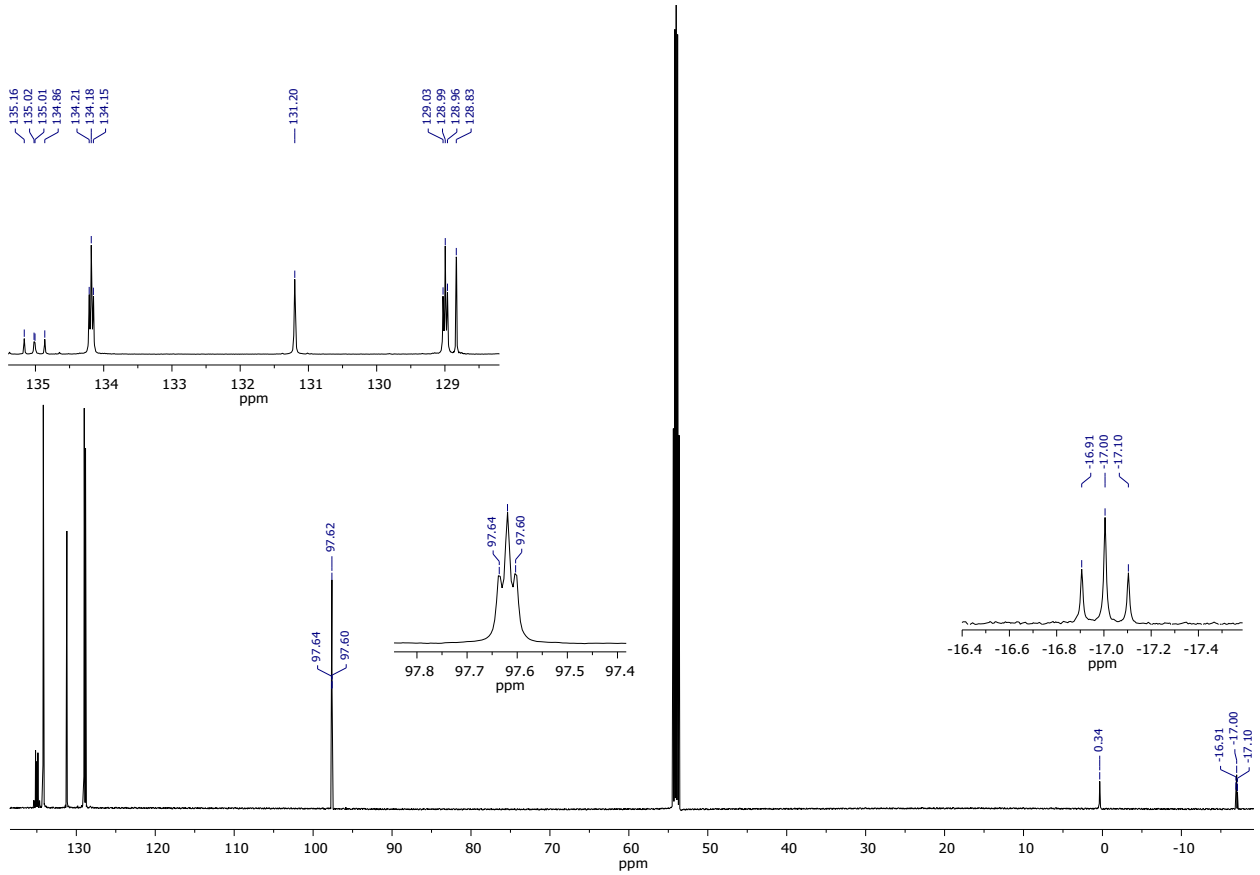

Figure S4. $^{13}C\{^{1}H\}$ NMR spectrum (151 MHz, CD_2Cl_2, 298 K) of [MeRu(h^6-C_6H_6)(PPh_3)$_2$][$GaMe_2Cl_2$].

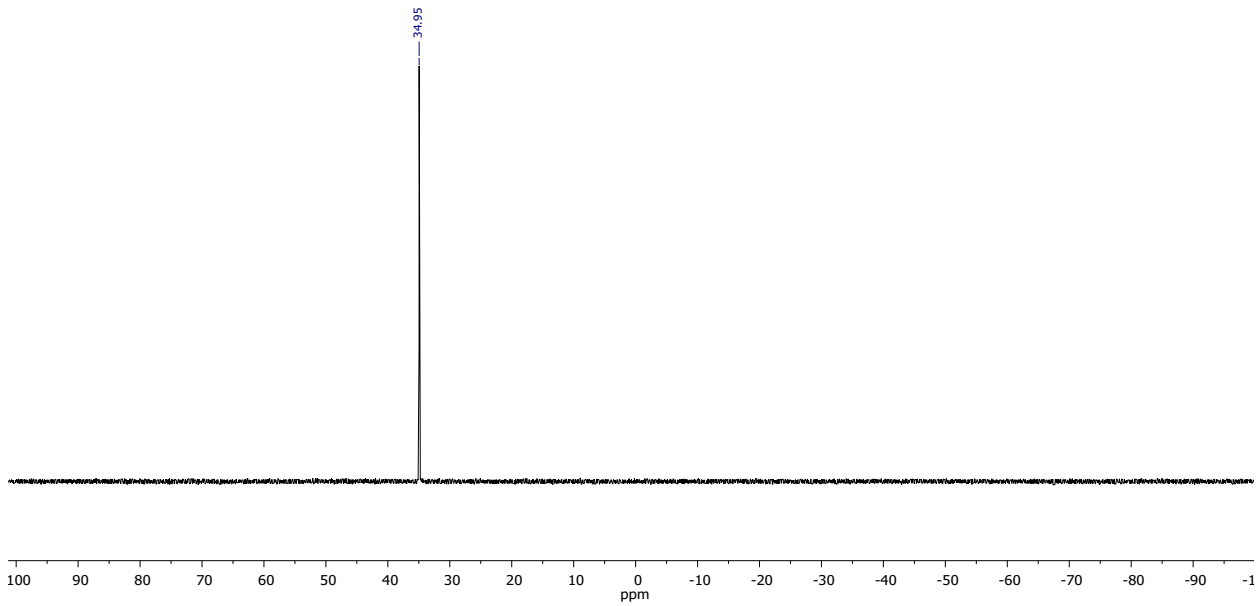

Figure S5. ^{31}P NMR spectrum (202 MHz, CD_2Cl_2, 298 K) of [MeRu(h^6-C_6H_6)(PPh_3)$_2$][$GaMe_2Cl_2$].

3. Single crystal X-ray diffraction

3.1 Crystal Structure Report for complex **1**

CCDC 2072598 contains the supplementary X-ray data which can be obtained free of charge from The Cambridge Crystallographic Data Center.

A yellow prism like single crystal of $C_{51}H_{51}Cl_2GaP_2Ru$, approximate dimensions (0.151 x 0.290 x 0.375) mm^3, was selected for the X-ray crystallographic analysis and mounted on a cryoloop using an oil cryoprotectant. The X-ray intensity data was measured at low temperature (T = 100K), using a three circles goniometer Kappa geometry with a fixed Kappa angle at = 54.74 deg Bruker AXS D8 Venture, equipped with a Photon 100 CMOS active pixel sensor detector. A monochromatized Mo X-ray radiation (λ = 0.71073 Å) was selected for the measurement.

Frames were integrated with the Bruker SAINT software package[7] using a narrow-frame algorithm. The integration of the data using a triclinic unit cell yielded a total of 86362 reflections to a maximum θ angle of 30.51° (0.70 Å resolution), of which 13617 were independent (average redundancy 6.342, completeness = 99.9%, R_{int} = 3.19%, R_{sig} = 2.10%) and 12366 (90.81%) were greater than $2\sigma(F^2)$. The final cell constants of a = 12.004(2) Å, b = 13.159(2) Å, c = 14.922(2) Å, α = 86.296(4)°, β = 87.495(6)°, γ = 71.750(4)°, volume = 2233.2(6) $Å^3$, are based upon the refinement of the XYZ-centroids of 2805 reflections above 20 σ(I) with 5.540° < 2θ < 50.57°. Data were corrected for absorption effects using the Multi-Scan method implemented in the program (SADABS).[8] The ratio of minimum to maximum apparent transmission was 0.867. The calculated minimum and maximum transmission coefficients (based on crystal size) are 0.6690 and 0.8430.

The structure was solved in a triclinic unit cell; space group: P -1, with Z = 2 for the formula unit, Z = 2 for the formula unit, $C_{51}H_{51}Cl_2GaP_2Ru$. Using the Bruker SHELXT[9] Software Package, refinement of the structure was carried out by least squares procedures on weighted F^2 values using the SHELXTL-2018/3[10] included in the APEX3 v2019, 1.0, AXS Bruker program.[11] Hydrogen atoms were localized on difference Fourier maps but then introduced in the refinement as fixed contributors in idealized geometry with an isotropic thermal parameters fixed at 20 % higher than those carbons atoms they were connected. A molecule of benzene was also found crystallized.

The final anisotropic full-matrix least-squares refinement on F^2 with 518 variables converged at R1 = 2.54%, for the observed data and wR2 = 5.79% for all data. The goodness-of-fit: GOF was 1.063. The largest peak in the final difference electron density synthesis was 0.789 $e^-/Å^3$ and the largest hole was -0.497 $e^-/Å^3$ with an RMS deviation of 0.069 $e^-/Å^3$. On the basis of the final model, the calculated density was 1.439 g/cm^3 and F(000), 992 e^-. Graphics were performed using softwares: Mercury V.4.2.0: (https://www.ccdc.cam.ac.uk/) and POV-Ray v 3.7: (The Persistence of Vision Raytracer, high quality, Free Software tool).

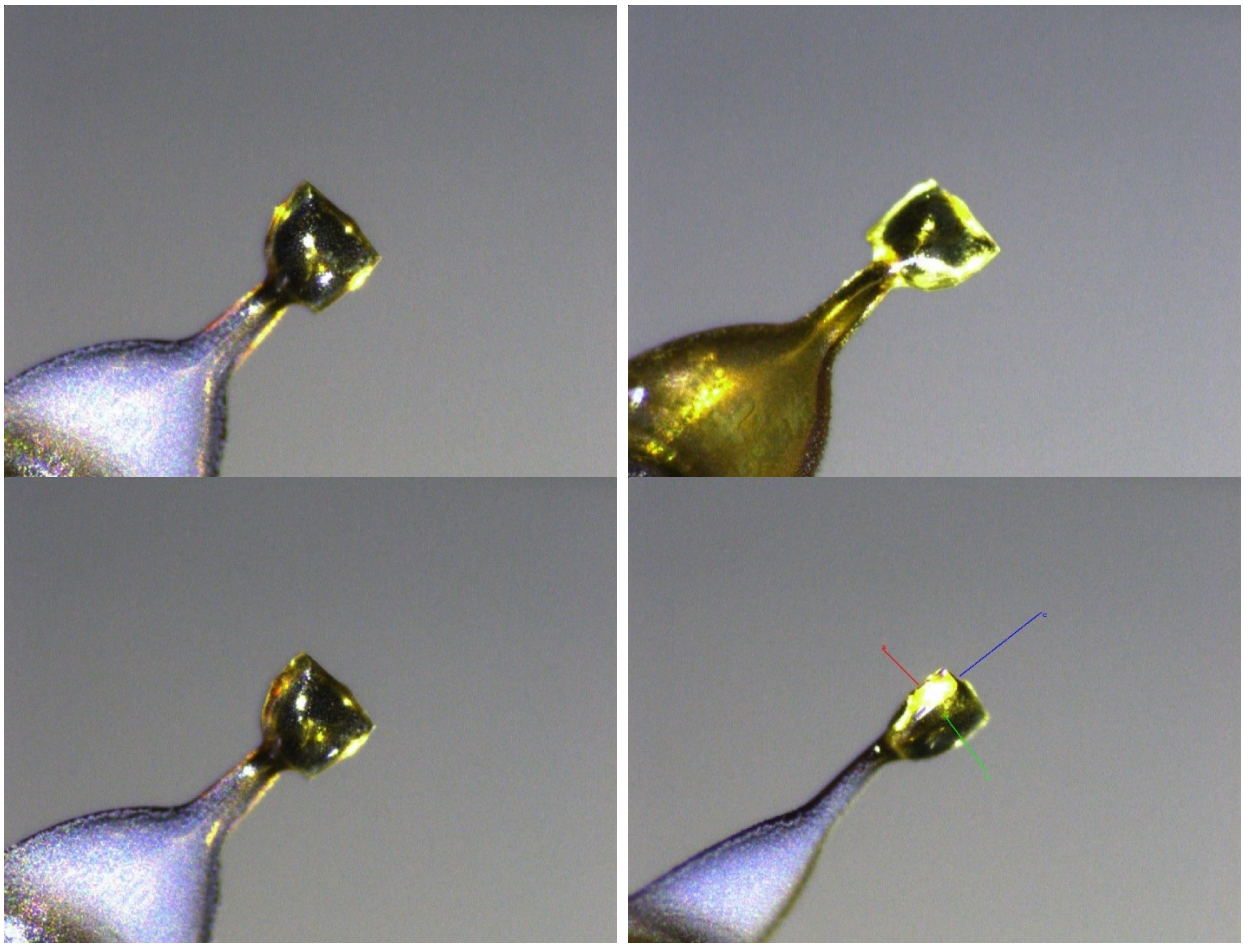

Figure S6. Crystals' view

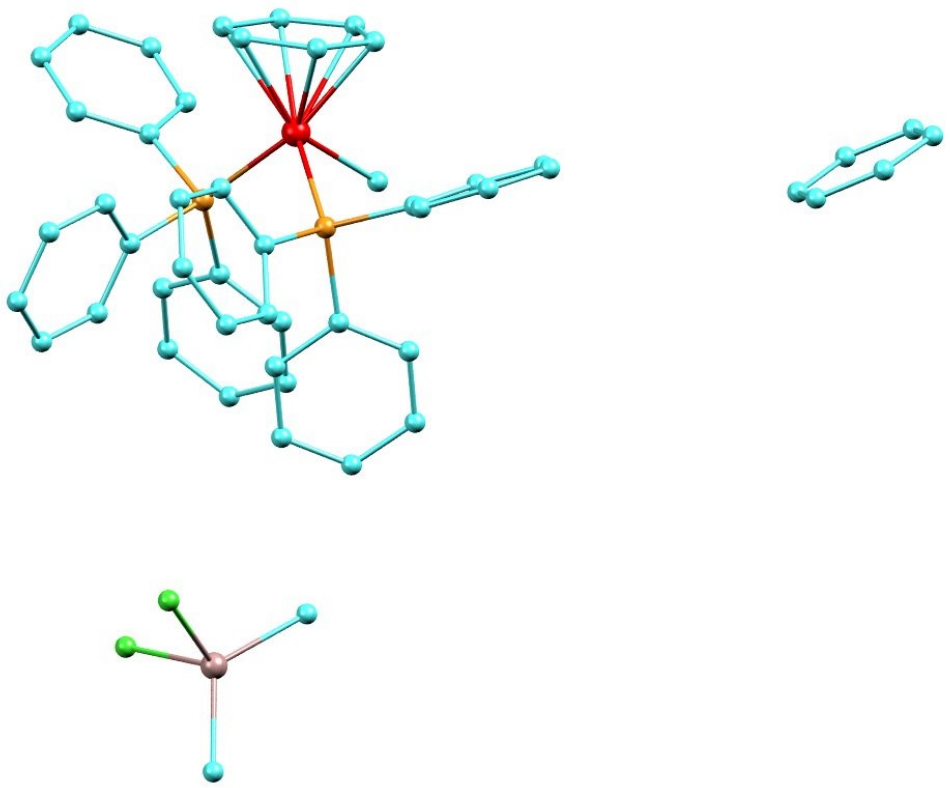

Figure S7. Asymmetric unit's view

Table S3. Sample and crystal data for B_VM_042.

Identification code	B_VM_042	
Chemical formula	$C_{51}H_{51}Cl_2GaP_2Ru$	
Formula weight	967.55 g/mol	
Temperature	100(2) K	
Wavelength	0.71073 Å	
Crystal size	(0.151 x 0.290 x 0.375) mm^3	
Crystal system	triclinic	
Space group	P -1	
Unit cell dimensions	a = 12.004(2) Å	α = 86.296(4)°
	b = 13.159(2) Å	β = 87.495(6)°
	c = 14.922(2) Å	γ = 71.750(4)°
Volume	2233.2(6) $Å^3$	

Z	2
Density (calculated)	1.439 g/cm^3
Absorption coefficient	1.167 mm^{-1}
F(000)	992

Table S4. Data collection and structure refinement for B_VM_042.

Theta range for data collection	2.28 to 30.51°	
Index ranges	-17<=h<=17, -18<=k<=18, -21<=l<=19	
Reflections collected	86362	
Independent reflections	13617 [R(int) = 0.0319]	
Coverage of independent reflections	99.9%	
Absorption correction	Multi-Scan	
Max. and min. transmission	0.8430 and 0.6690	
Structure solution technique	direct methods	
Structure solution program	XT, VERSION 2014/5	
Refinement method	Full-matrix least-squares on F^2	
Refinement program	SHELXL-2018/3 (Sheldrick, 2018)	
Function minimized	$\Sigma\ w(F_o^2 - F_c^2)^2$	
Data / restraints / parameters	13617 / 0 / 518	
Goodness-of-fit on F^2	1.063	
Δ/σ_{max}	0.002	
Final R indices	12366 data; I>2σ(I)	R1 = 0.0254, wR2 = 0.0553
	all data	R1 = 0.0308, wR2 = 0.0579
Weighting scheme	$w=1/[\sigma^2(F_o^2)+(0.0165P)^2+2.1604P]$ where $P=(F_o^2+2F_c^2)/3$	
Extinction coefficient	0.0077(3)	
Largest diff. peak and hole	0.789 and -0.497 eÅ^{-3}	
R.M.S. deviation from mean	0.069 eÅ^{-3}	

Table S5. Bond lengths (Å) for B_VM_042.

Ru1-C1	2.1559(14)	Ru1-C5	2.2509(14)
Ru1-C6	2.2662(14)	Ru1-C4	2.2685(14)
Ru1-C3	2.2950(15)	Ru1-C2	2.2974(14)
Ru1-C7	2.3442(14)	Ru1-P2	2.3496(4)
Ru1-P1	2.3703(4)	P1-C20	1.8354(13)
P1-C8	1.8434(14)	P1-C14	1.8436(14)
P2-C38	1.8274(14)	P2-C32	1.8357(14)
P2-C26	1.8458(14)	C1-H1A	0.98
C1-H1B	0.98	C1-H1C	0.98
C2-C7	1.404(2)	C2-C3	1.416(2)
C2-H2	0.95	C3-C4	1.400(2)
C3-H3	0.95	C4-C5	1.415(2)
C4-H4	0.95	C5-C6	1.411(2)
C5-H5	0.95	C6-C7	1.416(2)
C6-H6	0.95	C7-H7	0.95
C8-C9	1.3945(19)	C8-C13	1.4009(19)
C9-C10	1.399(2)	C9-H9	0.95
C10-C11	1.386(2)	C10-H10	0.95
C11-C12	1.392(2)	C11-H11	0.95
C12-C13	1.393(2)	C12-H12	0.95
C13-H13	0.95	C14-C15	1.3944(19)
C14-C19	1.4075(19)	C15-C16	1.3968(19)
C15-H15	0.95	C16-C17	1.387(2)
C16-H16	0.95	C17-C18	1.391(2)
C17-H17	0.95	C18-C19	1.3908(19)
C18-H18	0.95	C19-H19	0.95
C20-C21	1.3971(19)	C20-C25	1.4031(19)
C21-C22	1.388(2)	C21-H21	0.95
C22-C23	1.391(2)	C22-H22	0.95
C23-C24	1.389(2)	C23-H23	0.95
C24-C25	1.389(2)	C24-H24	0.95
C25-H25	0.95	C26-C31	1.401(2)
C26-C27	1.400(2)	C27-C28	1.395(2)

C27-H27	0.95	C28-C29	1.391(2)
C28-H28	0.95	C29-C30	1.379(2)
C29-H29	0.95	C30-C31	1.398(2)
C30-H30	0.95	C31-H31	0.95
C32-C33	1.389(2)	C32-C37	1.405(2)
C33-C34	1.390(2)	C33-H33	0.95
C34-C35	1.388(2)	C34-H34	0.95
C35-C36	1.384(3)	C35-H35	0.95
C36-C37	1.392(2)	C36-H36	0.95
C37-H37	0.95	C38-C39	1.393(2)
C38-C43	1.401(2)	C39-C40	1.398(2)
C39-H39	0.95	C40-C41	1.387(3)
C40-H40	0.95	C41-C42	1.389(3)
C41-H41	0.95	C42-C43	1.392(2)
C42-H42	0.95	C43-H43	0.95
Ga1-C44	1.9709(16)	Ga1-C45	2.0257(15)
Ga1-Cl2	2.2633(5)	Ga1-Cl1	2.2822(5)
C44-H44A	0.98	C44-H44B	0.98
C44-H44C	0.98	C45-H45A	0.98
C45-H45B	0.98	C45-H45C	0.98
C1S-C2S	1.377(2)	C1S-C6S	1.388(3)
C1S-H1S	0.95	C2S-C3S	1.383(2)
C2S-H2S	0.95	C3S-C4S	1.385(3)
C3S-H3S	0.95	C4S-C5S	1.392(3)
C4S-H4S	0.95	C5S-C6S	1.391(3)
C5S-H5S	0.95	C6S-H6S	0.95

Table S6. Bond angles (°) for B_VM_042.

C1-Ru1-C5	93.67(6)	C1-Ru1-C6	127.43(6)
C5-Ru1-C6	36.39(6)	C1-Ru1-C4	81.64(6)
C5-Ru1-C4	36.49(6)	C6-Ru1-C4	64.97(6)
C1-Ru1-C3	99.80(6)	C5-Ru1-C3	65.20(6)

C6-Ru1-C3	76.38(5)	C4-Ru1-C3	35.73(6)
C1-Ru1-C2	134.82(6)	C5-Ru1-C2	76.63(6)
C6-Ru1-C2	64.38(5)	C4-Ru1-C2	64.31(6)
C3-Ru1-C2	35.92(6)	C1-Ru1-C7	156.39(5)
C5-Ru1-C7	64.55(6)	C6-Ru1-C7	35.71(5)
C4-Ru1-C7	75.32(5)	C3-Ru1-C7	63.78(5)
C2-Ru1-C7	35.19(5)	C1-Ru1-P2	87.50(4)
C5-Ru1-P2	100.41(4)	C6-Ru1-P2	87.91(4)
C4-Ru1-P2	133.66(4)	C3-Ru1-P2	164.05(4)
C2-Ru1-P2	137.46(4)	C7-Ru1-P2	104.64(4)
C1-Ru1-P1	87.89(4)	C5-Ru1-P1	163.20(4)
C6-Ru1-P1	144.64(4)	C4-Ru1-P1	127.80(4)
C3-Ru1-P1	98.04(4)	C2-Ru1-P1	90.42(4)
C7-Ru1-P1	110.28(4)	P2-Ru1-P1	96.366(17)
C20-P1-C8	102.69(6)	C20-P1-C14	101.17(6)
C8-P1-C14	99.17(6)	C20-P1-Ru1	115.85(5)
C8-P1-Ru1	108.60(5)	C14-P1-Ru1	126.02(5)
C38-P2-C32	100.75(6)	C38-P2-C26	103.89(6)
C32-P2-C26	100.69(6)	C38-P2-Ru1	118.49(5)
C32-P2-Ru1	120.46(5)	C26-P2-Ru1	110.03(5)
Ru1-C1-H1A	109.5	Ru1-C1-H1B	109.5
H1A-C1-H1B	109.5	Ru1-C1-H1C	109.5
H1A-C1-H1C	109.5	H1B-C1-H1C	109.5
C7-C2-C3	120.72(14)	C7-C2-Ru1	74.22(8)
C3-C2-Ru1	71.94(8)	C7-C2-H2	119.6
C3-C2-H2	119.6	Ru1-C2-H2	126.0
C4-C3-C2	119.27(14)	C4-C3-Ru1	71.10(8)
C2-C3-Ru1	72.13(8)	C4-C3-H3	120.4
C2-C3-H3	120.4	Ru1-C3-H3	128.6
C3-C4-C5	120.92(14)	C3-C4-Ru1	73.16(8)
C5-C4-Ru1	71.08(8)	C3-C4-H4	119.5
C5-C4-H4	119.5	Ru1-C4-H4	128.5
C6-C5-C4	119.05(14)	C6-C5-Ru1	72.40(8)
C4-C5-Ru1	72.43(8)	C6-C5-H5	120.5

C4-C5-H5	120.5	Ru1-C5-H5	126.6
C5-C6-C7	120.61(14)	C5-C6-Ru1	71.21(8)
C7-C6-Ru1	75.15(8)	C5-C6-H6	119.7
C7-C6-H6	119.7	Ru1-C6-H6	125.7
C2-C7-C6	119.15(14)	C2-C7-Ru1	70.58(8)
C6-C7-Ru1	69.14(8)	C2-C7-H7	120.4
C6-C7-H7	120.4	Ru1-C7-H7	132.8
C9-C8-C13	118.78(13)	C9-C8-P1	123.66(11)
C13-C8-P1	117.47(11)	C8-C9-C10	120.41(14)
C8-C9-H9	119.8	C10-C9-H9	119.8
C11-C10-C9	120.27(14)	C11-C10-H10	119.9
C9-C10-H10	119.9	C10-C11-C12	119.85(14)
C10-C11-H11	120.1	C12-C11-H11	120.1
C11-C12-C13	119.93(14)	C11-C12-H12	120.0
C13-C12-H12	120.0	C12-C13-C8	120.73(14)
C12-C13-H13	119.6	C8-C13-H13	119.6
C15-C14-C19	118.47(12)	C15-C14-P1	123.35(10)
C19-C14-P1	117.83(10)	C14-C15-C16	120.58(13)
C14-C15-H15	119.7	C16-C15-H15	119.7
C17-C16-C15	120.33(13)	C17-C16-H16	119.8
C15-C16-H16	119.8	C16-C17-C18	119.83(13)
C16-C17-H17	120.1	C18-C17-H17	120.1
C17-C18-C19	120.02(13)	C17-C18-H18	120.0
C19-C18-H18	120.0	C18-C19-C14	120.76(13)
C18-C19-H19	119.6	C14-C19-H19	119.6
C21-C20-C25	118.49(12)	C21-C20-P1	117.66(10)
C25-C20-P1	123.84(10)	C22-C21-C20	121.05(13)
C22-C21-H21	119.5	C20-C21-H21	119.5
C21-C22-C23	119.88(13)	C21-C22-H22	120.1
C23-C22-H22	120.1	C24-C23-C22	119.74(13)
C24-C23-H23	120.1	C22-C23-H23	120.1
C25-C24-C23	120.44(14)	C25-C24-H24	119.8
C23-C24-H24	119.8	C24-C25-C20	120.38(13)
C24-C25-H25	119.8	C20-C25-H25	119.8

C31-C26-C27	118.28(13)	C31-C26-P2	121.71(11)
C27-C26-P2	119.96(11)	C28-C27-C26	120.70(14)
C28-C27-H27	119.7	C26-C27-H27	119.7
C29-C28-C27	120.26(14)	C29-C28-H28	119.9
C27-C28-H28	119.9	C30-C29-C28	119.67(14)
C30-C29-H29	120.2	C28-C29-H29	120.2
C29-C30-C31	120.46(15)	C29-C30-H30	119.8
C31-C30-H30	119.8	C30-C31-C26	120.62(14)
C30-C31-H31	119.7	C26-C31-H31	119.7
C33-C32-C37	118.54(13)	C33-C32-P2	120.61(11)
C37-C32-P2	120.47(11)	C32-C33-C34	121.07(14)
C32-C33-H33	119.5	C34-C33-H33	119.5
C35-C34-C33	119.98(15)	C35-C34-H34	120.0
C33-C34-H34	120.0	C36-C35-C34	119.78(14)
C36-C35-H35	120.1	C34-C35-H35	120.1
C35-C36-C37	120.40(15)	C35-C36-H36	119.8
C37-C36-H36	119.8	C36-C37-C32	120.23(15)
C36-C37-H37	119.9	C32-C37-H37	119.9
C39-C38-C43	119.15(13)	C39-C38-P2	122.67(11)
C43-C38-P2	118.10(11)	C38-C39-C40	120.08(15)
C38-C39-H39	120.0	C40-C39-H39	120.0
C41-C40-C39	120.20(16)	C41-C40-H40	119.9
C39-C40-H40	119.9	C40-C41-C42	120.18(14)
C40-C41-H41	119.9	C42-C41-H41	119.9
C41-C42-C43	119.77(15)	C41-C42-H42	120.1
C43-C42-H42	120.1	C42-C43-C38	120.58(15)
C42-C43-H43	119.7	C38-C43-H43	119.7
C44-Ga1-C45	122.85(8)	C44-Ga1-Cl2	106.10(5)
C45-Ga1-Cl2	109.10(5)	C44-Ga1-Cl1	109.41(6)
C45-Ga1-Cl1	104.65(6)	Cl2-Ga1-Cl1	103.06(2)
Ga1-C44-H44A	109.5	Ga1-C44-H44B	109.5
H44A-C44-H44B	109.5	Ga1-C44-H44C	109.5
H44A-C44-H44C	109.5	H44B-C44-H44C	109.5
Ga1-C45-H45A	109.5	Ga1-C45-H45B	109.5

H45A-C45-H45B	109.5	Ga1-C45-H45C	109.5
H45A-C45-H45C	109.5	H45B-C45-H45C	109.5
C2S-C1S-C6S	120.39(17)	C2S-C1S-H1S	119.8
C6S-C1S-H1S	119.8	C1S-C2S-C3S	120.03(16)
C1S-C2S-H2S	120.0	C3S-C2S-H2S	120.0
C2S-C3S-C4S	120.34(17)	C2S-C3S-H3S	119.8
C4S-C3S-H3S	119.8	C3S-C4S-C5S	119.63(17)
C3S-C4S-H4S	120.2	C5S-C4S-H4S	120.2
C6S-C5S-C4S	119.97(17)	C6S-C5S-H5S	120.0
C4S-C5S-H5S	120.0	C1S-C6S-C5S	119.63(17)
C1S-C6S-H6S	120.2	C5S-C6S-H6S	120.2

4. Powder X-ray Diffraction

Powder X-Ray Diffraction Patterns (PXRD) were collected on a Rigaku Diffractometer, Ultima IV with a Cu-Kα_1 radiation (λ = 1.5406 Å) using a nickel filter. Patterns were recorded in the 2-50° 2θ range with a step scan of 0.02° and 2 seconds per step.

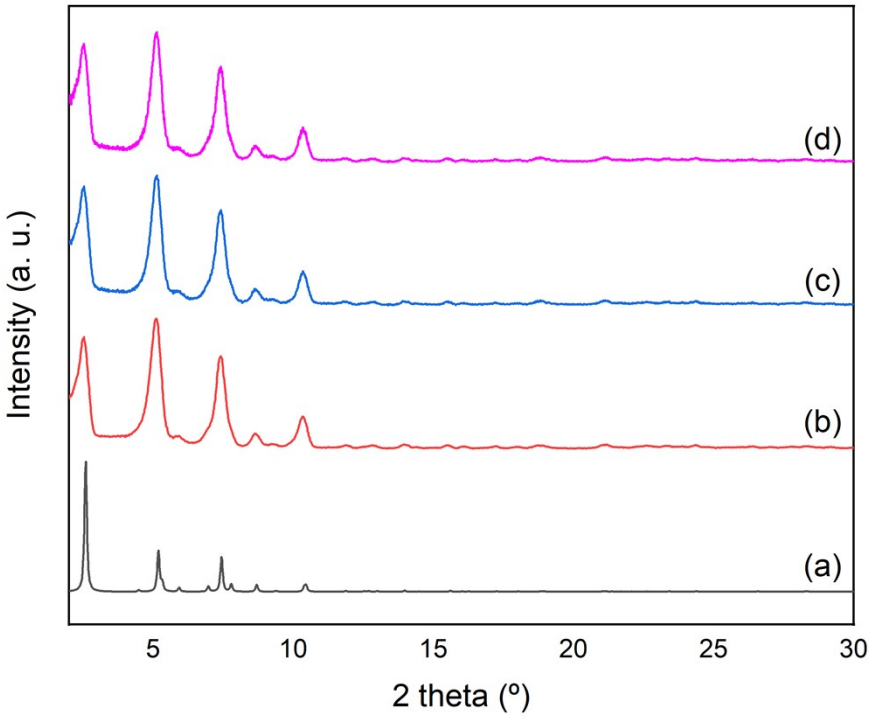

Figure S8. PXRD paterns of (a) simulated NU-1000, (b) [RuGa]@NU-1000, (c) [RuGa]@NU-1000 after SO_2 adsorption and (d) [RuGa]@NU-1000 after 10 SO_2 cycles

5. N_2 and SO_2 isotherms

N_2 isotherms (up to P/P_0 = 1 and 77 K) were recorded on a micromeritics ASAP 2020 analyser under high vacuum in a clean system with a diaphragm pumping system. Samples were thoroughly washed with acetone and acetone-exchange prior activation. Activation was carried out at 453 K under high vacuum using a turbomolecular pump for 16 h.
SO_2 isotherms were recorded at 298 K and up to 1 bar with the aid of a Dynamic Gravimetric Gas/Vapour Sorption Analyser, DVS Vacuum (Surface Measurements Systems Ltd.). Ultra-pure grade (99.9995%) N_2 and SO_2 were purchased from PRAXAIR.

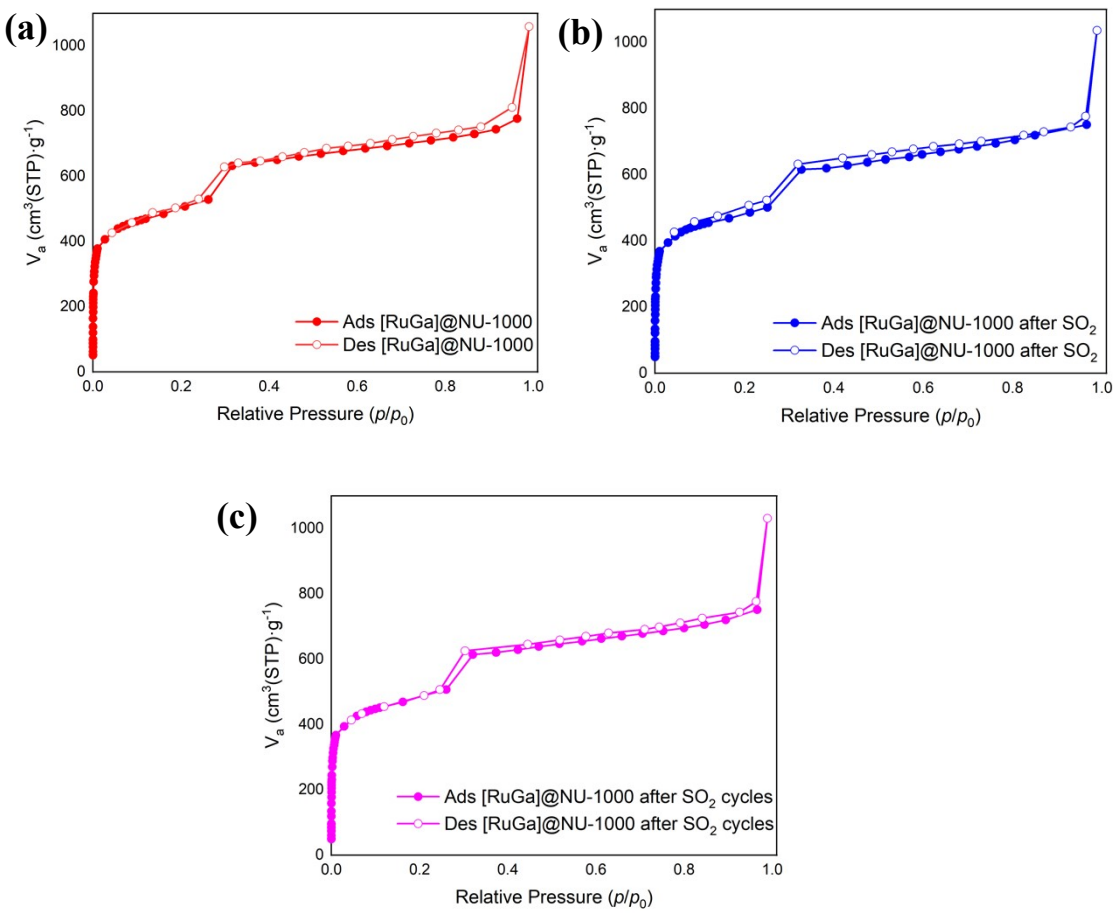

Figure S9. N_2 adsorption isotherms for (a) [RuGa]@NU-1000, (b) [RuGa]@NU-1000 after SO_2 adsorption and (c) [RuGa]@NU-1000 after ten SO_2 cycles

6. Heat of adsorption of SO_2

The heat of adsorption of SO_2, ΔH, was calculated by the isosteric method for NU-1000 and [Ir]@NU-1000, using the corresponding adsorption isotherms at three different temperatures, 298, 303 and 308 K (Figure S 15 and Figure S 16 A, C, E). A virial-type equation was used to fit the adsorption isotherms:

$$ln\left(\frac{n}{p}\right) = A_0 + A_1 n + A_2 n^2 + \cdots \qquad \textbf{Eq. S6.1}$$

where p is the pressure, n is the amount adsorbed and A_0, A_1, ... are the virial coefficients (A_2 and higher terms can be ignored at lower coverage values). A plot of $ln(n/p)$ versus n should give a straight line at low surface coverage (Figure S 15 and Figure S 16 B, D, F).

The obtained values and their average, -50.9 and –89.8 kJ mol^{-1} for NU-1000 and [Ir]@NU-1000, respectively, are reported on Table S4.

Table S7. Estimated heats of adsorption at three different temperatures 298, 308 and 318 K for [RuGa]@NU-1000

T [K]	Q_{est} [kJ mol^{-1}]
298 and 308	-110.16
298 and 318	-107.74
308 and 318	-96.14
Average=	**-104.68**

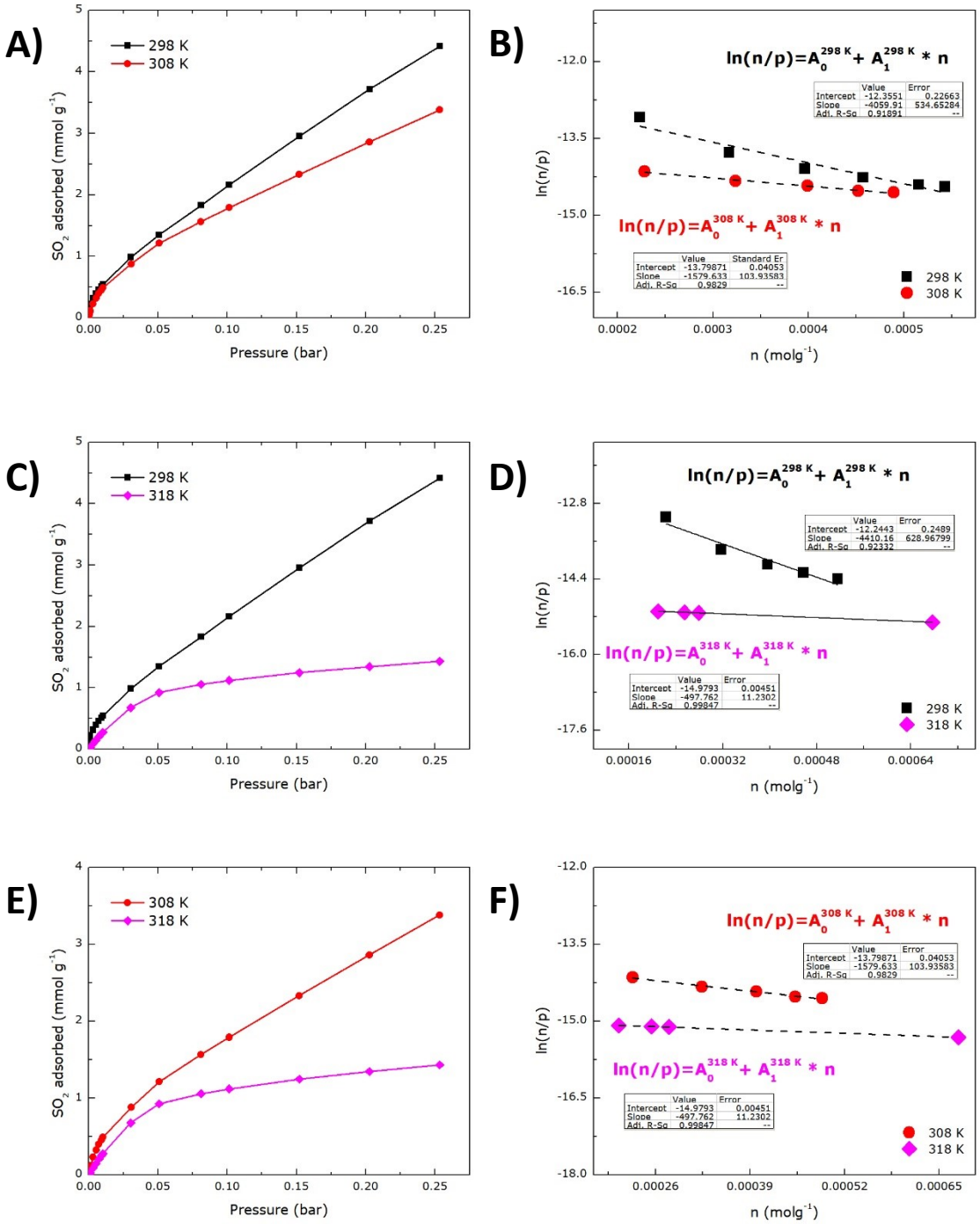

Figure S10. SO_2 adsorption isotherms at A) 298 and 308 K, C) 298 and 318 K, E) 308 and 318 K, for [RuGa]@NU-1000. Virial fitting plots at B) 298 and 308 K, D) 298 and 318 K, F) 308 and 318 K.

1. Hallman, P. S.; Stephenson, T. A.; Wilkinson, G., Tetrakis(triphenylphosphine)dichlororuthenium(II) and Tris(triphenylphosphine)dichlororuthenium(II). In *Inorganic Syntheses*, 1970; pp 237-240.
2. Abis, L.; Santi, R.; Halpern, J., Synthesis and characterization of some trans-hydridomethylbis(phosphine)-platinum(II) and -palladium(II) complexes. *Journal of Organometallic Chemistry* **1981,** *215* (2), 263-267.
3. Pankajakshan, A.; Sinha, M.; Ojha, A. A.; Mandal, S., Water-Stable Nanoscale Zirconium-Based Metal–Organic Frameworks for the Effective Removal of Glyphosate from Aqueous Media. *ACS Omega* **2018,** *3* (7), 7832-7839.
4. Bag, P. P.; Wang, X.-S.; Sahoo, P.; Xiong, J.; Cao, R., Efficient photocatalytic hydrogen evolution under visible light by ternary composite CdS@NU-1000/RGO. *Catalysis Science & Technology* **2017,** *7* (21), 5113-5119.
5. Schön, G., Auger and direct electron spectra in X-ray photoelectron studies of zinc, zinc oxide, gallium and gallium oxide. *Journal of Electron Spectroscopy and Related Phenomena* **1973,** *2* (1), 75-86.
6. Shen, J. Y.; Adnot, A.; Kaliaguine, S., An ESCA study of the interaction of oxygen with the surface of ruthenium. *Applied Surface Science* **1991,** *51* (1), 47-60.
7. Saint Program included in the package software: APEX3 v2019.1.0.
8. Bruker (2001).Program name.Bruker AXS Inc., Madison, Wisconsin, USA.
9. SHELXT-Integrated space-group and crystal-structure determination Sheldrick, G. M. Acta Crystallogr., Sect. A 2015, A71, 3-8.
10. SHELXTL Sheldrick, G. M. Ver. 2018/3. Acta Crystallographica. Sect C Structural Chemistry 71, 3 - 8.
11. APEX3 v2019, 1.0, AXS Bruker program.